Available online at www.sciencedirect.com
ScienceDirect
Journal of Nuclear Materials 356 (2006) 178–188
journal of nuclear materials
www.elsevier.com/locate/jnucmat

Structural stability and hardness of carburized surfaces of 316 stainless steel after welding and after neutron irradiation

K. Farrell *,[1], T.S. Byun

Metals and Ceramics Division, Oak Ridge National Laboratory, P.O. Box 2008, MS-6151, Oak Ridge, TN 37831, USA

Abstract

Surface hardening treatments offer promise of mitigating the threat of liquid cavitation pitting erosion at the interior surfaces of the austenitic 316 stainless steel vessel that will hold the liquid mercury target of the Spallation Neutron Source. One treatment is a commercial carburization process in which carbon is impregnated at low temperature at concentrations up to 6 wt% in supersaturated solid solution to depths of about 33 μm. The surface hardness of 316L steel is raised from 150 to 200$HV_{0.05}$ (micro-Vickers hardness number at a 50 g load) to 1000–1200$HV_{0.05}$. It is shown that during subsequent electron beam welding the supersaturated carburized layer in the heat affected zone decomposes to a tiered microstructure of carbide phases in austenite. The hardness of this complex decomposition microstructure is in the range 530–1200$HV_{0.05}$, depending on the exposure temperature, the local carbon level, and the size of the carbide particles. To test whether the carburized solid solution layer would break down under atomic displacements from proton and neutron irradiation in service, specimens of annealed and 20% cold-rolled 316LN steel were neutron irradiated to 1 dpa at 60–100 °C. No softening of the layer was detected. Rather, the hardness of the layers was increased by 2–12%, compared to increases of 81% and 43% for the annealed and 20% cold rolled substrate materials, respectively. Optical microscopy examinations of the surfaces of the as-carburized-and-irradiated specimens revealed no sign of decomposition attributable to irradiation.
Published by Elsevier B.V.

1. Introduction

The Spallation Neutron Source (SNS) under construction at the Oak Ridge National Laboratory (ORNL) [1,2] will be driven by a high energy pulsed proton beam striking a liquid mercury target. The target vessel will be constructed from 316LN austenitic stainless steel. This steel is known to have excellent resistance to general corrosion and to retain satisfactory ductility after irradiation. It is also quite compatible with mercury, and limited irradiation tests at low doses in contact with mercury have shown no signs of enhanced corrosion. Of greater concern for the SNS target is the threat of cavitational pitting erosion. This type of pitting might occur at the interior surfaces of the vessel due to collapse of cavities created in the mercury from stress waves generated by the proton beam pulses [1]. A similar type of liquid cavitation erosion is well known in hydraulic systems involving hydrofoils, pipelines, pumps and valves where perturbed

* Corresponding author. Tel.: +1 865 482 2354; fax: +1 865 574 0641.
E-mail address: p-k-f@comcast.net (K. Farrell).
[1] Retired from M&C Division, ORNL.

0022-3115/$ - see front matter Published by Elsevier B.V.
doi:10.1016/j.jnucmat.2006.05.027

water flow occurs [3,4]. In general, the greatest resistance to cavitation pitting is shown by those alloys that offer a combination of corrosion resistance, high strength (hardness), and toughness [3]. For the SNS, several techniques have been considered to mitigate the expected erosion. One technique that has shown good promise is a surface hardening treatment known as Kolsterising® [5].

Kolsterising® is the registered trade name of a proprietary surface carburization treatment for austenitic alloys provided by Bodycote Metal Technology Group. It is a process in which carbon is diffused into the surface of an annealed austenitic alloy at low temperature. Details of the process are not available, but according to Bodycote's promotional information the carbon penetrates to a depth of about 33 μm during a regular treatment. For convenience hereon we will refer to this treated region as the Kolsterised layer, or K layer. Within this layer, the infiltrated carbon is purportedly incorporated in supersaturated interstitial solid solution in the austenite phase of the steel, with a concentration of 6–7 wt%C at the surface, decreasing to the substrate value of about 0.05%C at 33 μm depth [5]. The lattice parameter of the affected austenite is markedly expanded at the surface and to a diminishing degree with depth, following the carbon concentration profile [5,6]. An expanded lattice will put the surface in a state of compressive stress and increase its hardness. Bodycote attributes the high hardness and toughness of the K layer to the lattice expansion. Many of the features of the Kolsterising® treatment claimed for 316 stainless steel and other austenitic alloys have recently been confirmed for the heat of 316LN steel intended for use as the SNS mercury vessel [6]. Exceptions were that some iron carbide phase was found at the immediate surface, and the lattice expansions and carbon concentrations in the austenite phase of the K layer were not as large as those claimed for other grades of austenitic steels. Nevertheless, the surface hardness and hardness-depth profiles were the same as those reported for Bodycote's austenitic materials.

The expanded lattice and large supersaturation of carbon in the Kolsterised surface, assumed to be responsible for the remarkable hardness of the K layer, will not be in equilibrium outside the Kolsterising® environment. Conditions encountered during subsequent processing or in service that could cause atomic movements in the layer, such as heat from fabrication welding or the atomic displacements caused by irradiation with high energy protons and spallation neutrons, might induce the layer to decompose and lose its hardness and, presumably, its resistance to cavitation pitting. Indeed, Bodycote cautions against exposing Kolsterised parts to temperatures >500 °C and recommends that any welding should be done prior to the surface hardening treatment [5]. Thermal decomposition of the K layer will undoubtedly occur in the vicinity of fusion welds where the temperatures in the weld metal and the immediate heat-affected zone (HAZ) will certainly exceed the Kolsterising® temperature. But published information does not seem to be available on details of the thermal decomposition and it is not known to what extent such thermal decomposition will affect the desired high hardness. During fabrication of the SNS target vessel some welds will need to be made after the Kolsterising treatment, so it is essential to explore the welding response of a K layer.

Radiation-induced instability is more subtle than thermal decomposition, and because of the high concentrations of vacancies introduced by the irradiation it can occur at lower temperatures. Normally at the operating temperature of the mercury target, about 100 °C, irradiation with protons or neutrons will be expected to cause hardening of the stainless steel vessel. But irradiation can soften a material that has previously been hardened by other mechanisms [7–9]. Irradiation may cause stress relief, decomposition of metastable solid solutions, and changes in the nature of second phases. To determine whether these instability concerns are warranted for a K layer on the SNS target vessel, and to gauge the degree of any associated surface softening, the effects of welding and neutron irradiation have been investigated in Kolsterised specimens of 316L and 316LN stainless steels and are reported herein.

2. Experimental

Two sets of experiments were made, one on weldments and the other on irradiated specimens. For the welds, strip specimens 75 mm long × 25 mm wide, were cut from 2.5 mm and 3.2 mm thick walls of the channels in a full-size prototype of the nose of the SNS target vessel that had been Kolsterised by Bodycote in a regular 33 μm treatment. This prototype was machined from a mill-annealed block of 316L stainless steel. It was Kolsterised on all exposed surfaces, including open-ended internal channels. For welding, each strip was clamped

between tungsten blocks set about 13 mm apart in the vacuum chamber of an electron beam (EB) welder, and a penetration weld bead was made in a single pass along the center line between the blocks. Details of the weld procedure, and a broader description of the findings for the welds, are available in Ref. [10]. In the present paper, the microstructural changes and associated hardness changes in the K layer are summarized for a weld made in a 3.2 mm thick plate. The voltage was 125 kV and the current was started at 7.0 mA, which gave about 90% penetration, and was shortly raised to 7.3 mA to give full penetration for a while then reduced to 7.0 mA for the remainder of the weld bead. The travel speed was 4.2 mm/s. The vacuum was better than 10^{-4} Torr. These weld parameters are typical of those normally used for stainless steel of this thickness.

Microstructures were examined on polished-and-etched cross-sections through the weld. Hardness tests were made on the as-welded plate surfaces with no further preparation. To determine the hardness of a 33 μm thin layer, diamond indentation hardness measurements must be made at low load (50 g) to avoid the indenter protruding through the hardened skin into the softer substrate. At 50 g the diagonal lengths of the Vickers pyramidal impressions on as-Kolsterised surfaces are about 10 μm, which is less than one third of the thickness of the K layer. Therefore, the measured hardness values of about 1000–1200$HV_{0.05}$ are believed to be closely representative of the strength of the hardened surface layer.

In cross-sections through the skin the hardness declines to <200$HV_{0.05}$ at 35–40 μm depth, consistent with that of the untreated annealed austenite substrate. The hardness measurements were made manually with a Vickers diamond indenter at 50 g load and 15 s dwell time in a LECO M400-H2 machine.

For the irradiation tests, the specimens consisted of a number of disks 3 mm diameter × 0.25 mm thick intended for transmission electron microscopy and on-face hardness tests, and 1 mm wide slivers cut from TEM disks for use in optical metallography and through-section hardness tests. These specimens were prepared from 316LN steel in an annealed condition and in a 20% cold worked (20% CW) condition. Annealing treatments were performed at 1050 °C for 30 min in a vacuum furnace, and samples were furnace cooled after the annealing. All samples were mechanically polished on one surface to a mirror finish with a 0.25 μm diamond slurry and were Kolsterised on all surfaces in a regular 33 μm treatment. The disk and sliver specimens, including non-Kolsterised ones, were irradiated in the High Flux Isotope Reactor (HFIR) at ORNL to a fast neutron fluence of 1.2×10^{25} n/m^2 ($E > 0.1$ MeV), corresponding to a displacement dose of about 1 dpa. During irradiation the test pieces were contained in aluminum capsules that were perforated to admit flowing water coolant in contact with the specimens and keep them at a temperature of 60–100 °C.

The irradiated specimens were tested in a hot cell using an automatic micro-Vickers hardness testing system (Mitsutoyo AAV-500) at 50 g load and 10 s dwell time. Five or six hardness measurements were made for each specimen, and the duration time at constant load in each test was 10 s. Optical surface microstructures were observed on the irradiated specimens using the microscope of the hardness testing system, and the images were saved to electronic files. To date, hardness tests and metallographic examinations have been made only on the originally polished surfaces of the irradiated disk specimens with no further surface preparation for the tests.

3. Results

3.1. Welded specimens

Usually no structure is visible in a polished-and-etched cross-section of a K layer because it is highly resistant to etching; normally it is revealed as a featureless (white) band in contrast to the darkened, etched substrate. That etching response was reversed after the welding treatment, as shown in Fig. 1(a)–(c), which depict cross-sections at the top surface of the plate. The white arrows indicate the 33 μm depth of the original K layer. It is clear that the formerly plain white Kolsterised region was etched before any structure was visible in the substrate. Such speedy etching indicates reduced resistance to acid corrosion, consistent with thermally-induced decomposition of the layer. The microstructures in the layer varied considerably with degree of heating. They are described in detail in Ref. [10]. For the present purposes of demonstrating thermal decomposition of the K layer during welding, and investigating whether it reduces surface hardness, the example microstructures in Fig. 1 are sufficient to illustrate the range of decomposition structures encountered in the heat affected

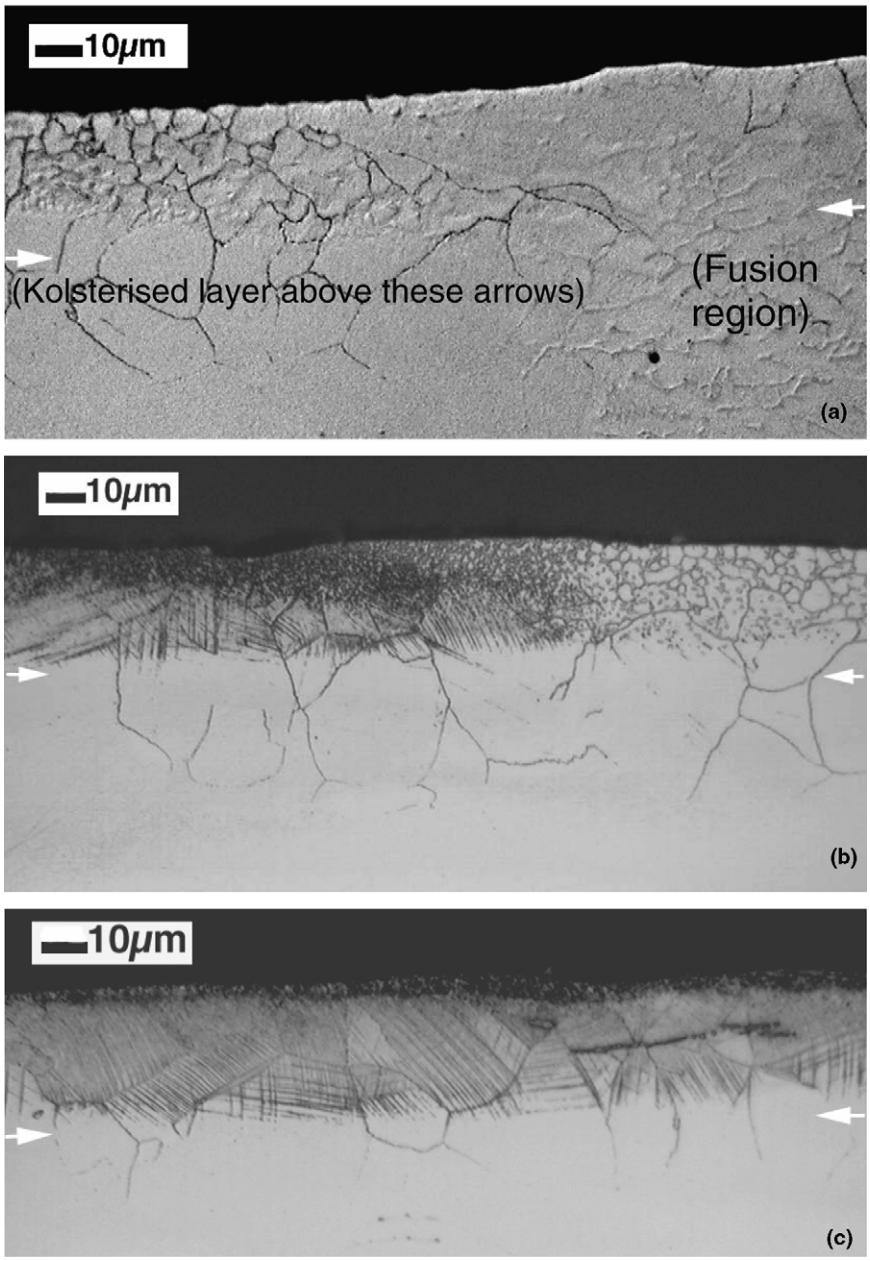

Fig. 1. Microstructures of cross-section through the weld and HAZ at the top of welded Kolsterised plate; (a) at the fusion line, (b) at about 2 mm to the left of the fusion line, and (c) at about 3 mm from fusion line.

zone (HAZ). In the weld bead, no signs of the former K layer were seen and the hardness was 150–200$HV_{0.05}$, the same as the substrate hardness.

In the HAZs at the top surface of the plate the microstructures were identical for the partial penetration weld and the full penetration weld. The field of Fig. 1(a) is located immediately to the left of the fusion line; here the vague cellular structure running from top to bottom at the right hand side of the photograph is the partially etched weld metal. This light etching in the weld metal is due to the presence of a small quantity of δ ferrite phase which is a normal component in autogenous welds made in austenitic stainless steel, and is more prone to etching than its matrix γ austenite phase. No structure corresponding to residue of a K layer was found at the surface layer of the weld metal. In the HAZ to the left of the fusion line, the K layer on the

substrate is seen as two tiers consisting of an outer tier of a somewhat cellular duplex structure with a cell size of 3–5 μm stretching from the surface to a depth of about 25 μm at which it terminates rather abruptly. Underlying this tier of fine cells, and partially obscured by it, are filaments of a coarser cell structure of 16–20 μm diameter, penetrating to a depth of about 60 μm. Deeper etching to expose the substrate reveals that the coarse cell structure lies on the parent metal austenite grain boundaries. This two tier arrangement of the K layer persists to a distance of several mm perpendicularly from the fusion line where it changes to a three-tier arrangement, as shown in Fig. 1(b). The change involves primarily the 25 μm thick tier which divides into an outer tier of very small cells and an under layer of a lamellar structure. The lamellar structure reaches a depth of about 25 μm and it changes orientation at the austenite grain boundaries. At a distance of about 3 mm from the fusion line, Fig. 1(c), the outer layer of fine cell structure was reduced to a crust about 3 μm deep in which the cells were further reduced and were barely discernable at the resolution limit of about 1 μm in these observations. The lamellar structure was more prominent and remained confined to a depth of about 25 μm. The penetration depth of the coarse cell structure was less than 50 μm. An inclusion stringer encompassed in the K layer at the upper right side of the field was deeply etched, as were other stringers elsewhere in the K layer. Stringers in the substrate were just barely visible. The structures in Fig. 1(c) were continuous across the top surface of the plate to a distance of 6.5 mm from the weld centerline at which the clamp blocks were located and where observations were considered to be compromised by the blocks.

On the underside of the full penetration portion of the weld, the decomposition microstructures were generally similar to those on the top face, except at the fusion lines on the bottom surface where the dripping weld bead tended to spread over the surface (see Ref. [10] for details of this enhanced wetting). On the underside of the partial penetration portion of the weld there was no fusion line and the microstructures in the K layer consisted of the 25 μm deep tier of 3–5 μm size duplex cell (austenite plus carbide) structure in the hottest regions directly below the base of the weld metal. Only a few traces of lamellar structure were seen, just below the 25 μm depth. In the cooler regions farther from the weld, a heavily dotted structure prevailed from which poked fingers of lamellar structure. An additional feature consisting of linear clusters of black, oval- or lenticular-shaped particles or cavities was found lying on the interior front of the 3–5 μm cell tier. These clusters occurred discontinuously and were seen only in the hotter regions below the weld. They are shown in Fig. 2 and are discussed in detail in Ref. [10].

Hardness values from traverses made on the K surfaces at three locations are displayed in Fig. 3. Traverse A was made on the top surface of the full penetration portion of the weld. Traverse A begins at the terminus pool of the weld bead and runs in the direction of the weld axis but away from the weld pool into unwelded metal. At this location the heat from the weld is the least because there was no weld pass and no plasma. The traverse A hardness data show that in the immediate HAZ at the pool fusion line the hardness has fallen from the as-Kolsterised value of 1000–1200$HV_{0.05}$ to about 600$HV_{0.05}$. At an axial distance of approximately 1 mm from the pool, the hardness is almost

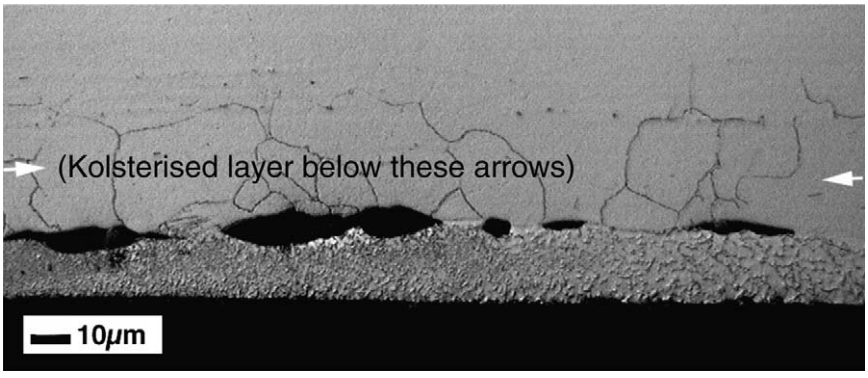

Fig. 2. Cross-section through the HAZ below a 90% penetration weld.

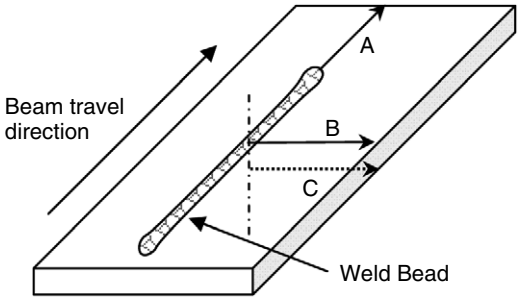

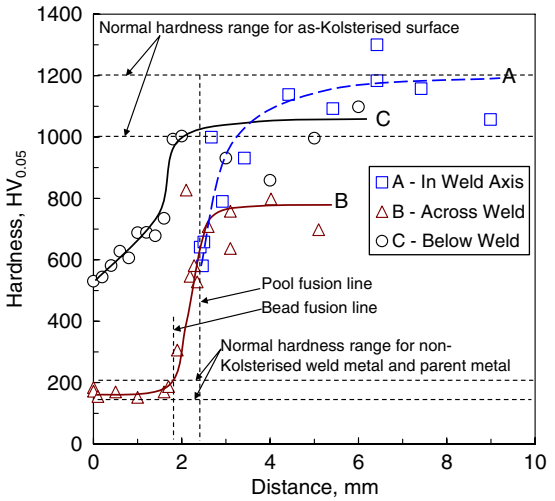

Fig. 3. Hardness traverses on surfaces of as-welded specimens at three locations.

within the scatter band for the as-Kolsterised condition, and it is certainly within the band at 2 mm distance. Efforts to obtain reliable hardness data within the frozen pool metal were defeated by the sunken and rippled surface. However, the hardness values in the pool are presumably the same as those illustrated for the weld metal region of traverse B, which fall in the band of 150–200$HV_{0.05}$ for non-Kolsterised weld metal and parent metal.

The region of traverse B received the largest heat input of all three traverses. Traverse B is made on the top surface of the partial penetration portion of the weld. It begins at the center of the weld bead and runs across it perpendicular to the bead axis, towards the clamps. Although the weld in traverse B was made with slightly less current than the full penetration portion of the weld, it certainly saw more power input, and thus more heat, than the route of traverse A, which saw no current. Additionally, it was preheated by the approaching weld spot, received reflected heat from the clamps, and inherited some tailgate heat from the heated clamps. The weld metal part of traverse B shows no residual hardness effects of the K treatment; the hardness of the weld is 150–200$HV_{0.05}$, which is the same as that for the non-Kolsterised parent metal. In the far HAZ regions of traverse B at distances beyond about 1 mm from the bead fusion line out to the clamp location the hardness of the K layer is reduced to about 700$HV_{0.05}$. In the near HAZ at distances <1 mm from the line, the hardness falls to <200$HV_{0.05}$.

Traverse C was also made in the partial penetration portion of the weld in the same direction as B but on the underside of the plate. Here, the surface beneath the weld was not melted. The area of traverse C saw less heat input than traverse B, but more than traverse A. The zero distance position for traverse C corresponds to the projected center line of the weld bead directly below the weld root. There, the hardness of the K layer was reduced to 530$HV_{0.05}$. It rose to 1000$HV_{0.05}$ at a distance of about 2 mm from the zero position.

A hardness trace was also made through the thickness of the K layer on a polished-and-etched cross-section of the weld bead at a distance of 5mm from the center line of the weld. At that position, the on-surface hardness was taken to be 700$HV_{0.05}$, corresponding with the 5 mm value for traverse B in Fig. 3. The results are presented in Fig. 4 where they are compared with cross-section

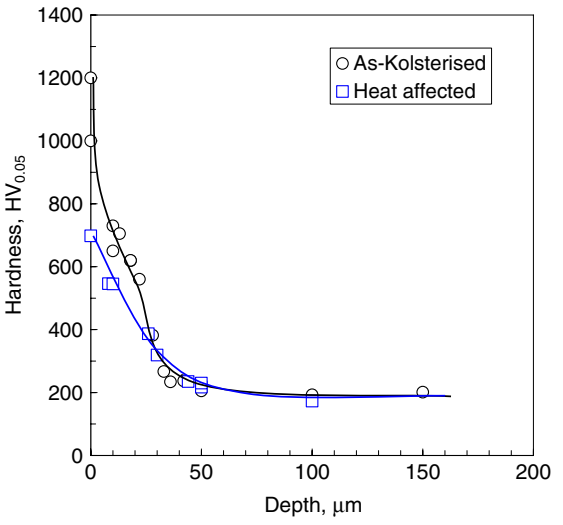

Fig. 4. Hardness–depth profiles for as-carburized and HAZ (at 5 mm from center of weld) conditions.

data measured on a Kolsterised unwelded plate cut from the same nose piece [6]. At shallow depths, within the carbon-rich region, the hardness values of the heat-affected K layer are less than those of the as-Kolsterised layer. At depths of 25 μm and beyond, the two curves merge.

3.2. Irradiated specimens

Optical metallographic examinations of the irradiated specimens were made in conjunction with hardness testing. It was noted that some patches of rust or surface contamination had occurred during irradiation or storage. Otherwise, no evidence of surface modification or breakdown of the K layer was found. At the hardness impressions, which ranged in diagonal length from about 25 μm in the as-annealed condition to about 9.5 μm in the Kolsterised conditions, Fig. 5, considerable plastic deformation occurred during indentation without causing cracking or flaking, indicating that the K layer remained tough despite irradiation.

On-face hardness values for the irradiated specimens are summarized in Fig. 6. Irradiation

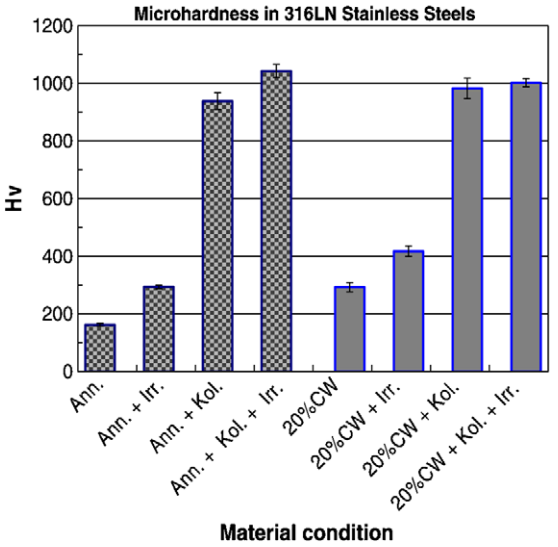

Fig. 6. Comparison of micro-hardness data for different material and surface conditions.

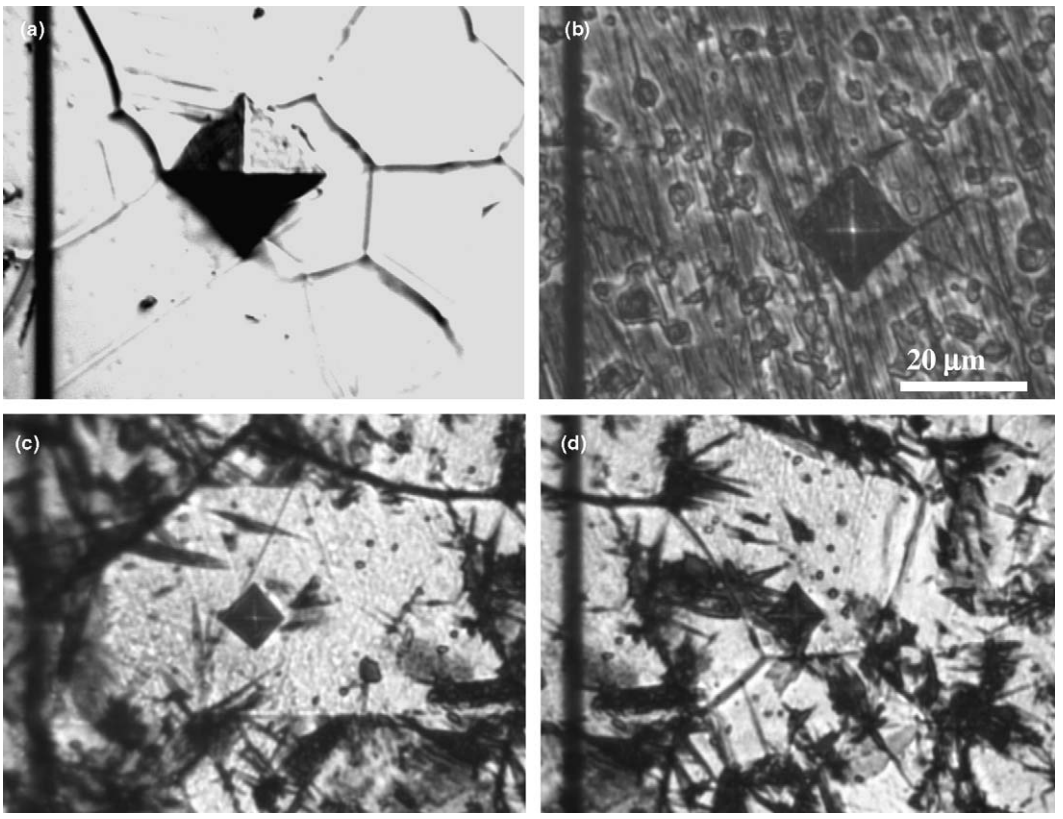

Fig. 5. Microstructures and indentation impressions in the annealed materials in (a) as-annealed, (b) annealed + irradiated, (c) annealed + Kolsterised, and (d) annealed + Kolsterised + irradiated conditions.

increased the hardness for all the starting conditions. The annealed material without Kolsterising® treatment showed the biggest increase in hardness by irradiation, about 81% increase from $162HV_{0.05}$ before irradiation. The hardness of the K layer on the annealed substrate was $939HV_{0.05}$ before irradiation, which is 5.8 times higher than that of the as-annealed surface. After irradiation, the K layer was hardened by about 11% to $1043HV_{0.05}$. In the 20% CW material, the hardness before irradiation was already about 80% higher than the annealed material, and it increased about 43% to $417HV_{0.05}$ after irradiation. The hardness in the as-Kolsterised 20% CW material was $983HV_{0.05}$, which was increased a mere 2% to $1002HV_{0.05}$ by the irradiation. This small increase is within the experimental error bounds for the Kolsterised 20% CW material before irradiation.

4. Discussion

4.1. Welded specimens

The hardness measurements and metallographic studies of the welded Kolsterised plate demonstrate unequivocally the thermal instability of the K layer. The degrees of softening shown in Fig. 3 are qualitatively consistent with the expected degrees of heat input at the locations of the various hardness traces. But the metallographic examinations show that hardness changes alone are not a sufficient indicator of decomposition of the K phase.

From Fig. 3 it is clear that all signs of the formerly high hardness of the K layer were erased in the molten weld metal portion of the weld pass. On the upper surface of the plate, in the immediate HAZs of traces A and B closest to the fusion line, the hardness is markedly reduced, more so in B than in A. At distances beyond 1–2 mm from the line, trace A which represents the least heat input displays no loss in hardness. Trace B, which represents the most heat input, portrays reduced hardness of about $750HV_{0.05}$ out to distances of about 6 mm where the clamp is positioned. Trace C, made on the bottom surface of the plate below the non-penetrating portion of the weld, is expected to have a heat input closer to that of trace A than that of trace B. In trace C, the 0–2 mm region below the weld root is the effective near-weld HAZ. There, the reduced hardness is 500–700 $HV_{0.05}$, which is comparable with that of the immediate HAZ of trace A. At distances in trace C beyond 2 mm the hardness is perhaps a little less than at comparable distances in trace A, and both fall in the scatter band for the as-Kolsterised condition. Metallographic observations reveal no evidence of the former K layer in the molten weld metal. They verify the expected thermal decomposition of the K layer in the high temperature regions of the HAZ closest to the fusion line, where large decreases in hardness were found. They also show that considerable fine-scale thermal decomposition occurs in the cooler regions of trace C at distances >2 mm from the projected weld center where no significant decreases in hardness are found. Obviously, a surface hardness measurement is not a reliable indicator of thermal decomposition of the K layer. The nature, and particularly the size, of the decomposition products are thought to be controlling factors, as discussed shortly.

No attempt was made to identify the decomposition products by in situ chemical analysis techniques. However, in Ref. [10] phase equilibria calculations indicate the most likely products will be carbon-depleted austenite and two carbide phases, $M_{23}C_6$ and M_7C_3. Some iron carbide may intrude at carbon concentrations above 4% and temperatures below 800 °C. The relative portions of these phases vary with carbon content and temperature and will therefore be different in a complex manner at the different carbon concentrations through the carbon gradient of the K layer and within the temperature gradients surrounding the weld. The M_7C_3 phase is expected to be most prominent at the higher temperatures and higher carbon levels. Of course, in the short time frame of a weld pass, thermal equilibrium will not be obtained over the whole heated area. Nevertheless, the phase calculations provide a reasonable guide to the nature of the thermal decomposition products. The calculations also indicated that the high carbon levels in the K layer will reduce the melting point of the layer by 200–300 °C.

The experimentally observed morphologies and spatial distributions of the decomposition products in the K layer are associated not only with the carbon gradient and the local temperature but also with microstructural features that existed in the layer before welding. Addressing first the spatial distribution; the decomposition products are found to be arranged in one to three overlaying strata lying parallel to the surface and, therefore, they probably correspond to different concentrations of carbon in the carbon depth profile. Stratum #1 is the duplex

cellular microstructure with a cell size that changes from about 5 μm in the hotter regions of the HAZ to ≪1 μm in the cooler regions. In the hottest regions of the HAZ it is the dominant structure. In cooler regions it lies only in a 3 μm thin crust at the outer surface where the carbon concentration is highest. Stratum #2 is the lamellar structure that penetrates to a uniform depth of 25–30 μm and is relatively insensitive to heat level. The lamellar structure exists in the cooler parts of the HAZ, and is not found in association with the 3–5 μm cells of stratum #1. This lamellar structure has the characteristics of slip lines from plastic deformation. The lines change orientation at the austenite grain boundaries. It is known that the Kolsterising® treatment causes plastic deformation of the surface of stainless steel, as evidenced by the formation of slip lines on the surface [6,10]. These slip lines are not visible in cross-sections cut through the as-Kolsterised layer because the layer does not etch easily. Therefore, it was not known how deep the lines penetrated below the surface. In the present work they are revealed because of decoration by small carbides under the influence of heat from the weld. Generally, these slip lines do not penetrate the full depth of the former 33 μm K layer, but occasionally a few are seen below the 33 μm depth in large grains that span the K layer and the immediate substrate.

Stratum #3 is the coarse network structure that lies on the parent austenite grain boundaries and penetrates to about twice the depth of the former K layer. At depths within stratum #3 beyond the lamellar band there are no visible decomposition products inside the austenite grains and, as seen in Fig. 3, the hardness is the same as for the substrate. Hence, the decorated austenite grain boundaries of stratum #3 do not contribute to surface hardness. The depth of stratum #3 indicates preferred penetration of carbon along the austenite boundaries to approximately twice the depth of the main K front. Such advanced infiltration has not been reported hereto for the Kolsterising® treatment. No effort was made to determine unambiguously whether it occurred during the Kolsterising® treatment or during heating from the weld. However, the position of the front of stratum #3 was seemingly independent of heat level in the HAZ, which would imply that the preferred penetration of carbon along the grain boundaries occurred during the K treatment.

The interpretation of the morphologies of the decomposition products is limited by the resolution limit of about 1 μm in these optical examinations at which a particle could be discerned as a dot, but below which the particles were a just a grayish haze. The decorations on austenite grain boundaries and slip lamellae were hazy. In the small cells of 3–5 μm size the cells were mostly contiguous and their boundaries were quite thick. Islands were present in the larger ones. Because these cells are associated only with the hottest regions of the HAZ and they lie in the higher carbon regions of the K layer where the phase equilibrium calculations identified M_7C_3 phase as the major decomposition product, it is presumed that they are a mix of M_7C_3 phase and austenite. A noteworthy feature of these 3–5 μm cells is that although they overlap the 25 μm deep plastically deformed band of the K layer the cells contain no evidence of slip lines. The implication is that the former slip bands from the K treatment were erased by thermally-induced formation of the cells during welding. It is proposed that the cellular morphology of the cells might be due to local recovery and recrystallization in the former slipped region of the heated K layer. The cell boundaries and islands are assumed to be M_7C_3 phase. Such local recrystallization could be aided and abetted by the carbon-reduced melting temperature of the most carbon-rich regions of the K layer. In the very-near HAZs momentary melting and freezing of the most carbon-rich regions could occur at temperatures too low to melt the substrate but above the reduced melting temperature of the K layer. Elsewhere, in the unmelted regions, the reduced melting temperatures of the carbon rich layer will favor solid state thermal recovery and recrystallization and the formation of carbides in the hotter regions. These processes are assisted by vacancies. Since the thermal vacancy concentration scales with the ratio of the actual temperature to the melting temperature, a carbon-reduced melting temperature will cause more vacancies to be produced at a given actual temperature. In cooler regions of the HAZ where the fine, hazy structure dominates, the lamellar structure is probably not destroyed but is largely hidden by the high density of fine carbides.

The final consideration for the welds, and perhaps the most important one, is the relationship between weld-associated thermal decomposition of the K layer and surface hardness. A conclusion from this work is that hardness measurements alone are not a satisfactory means of determining whether decomposition has occurred. It is found that the hardness of the K layer can be totally eliminated,

partially reduced, or not affected, depending on the nature and scale of the decomposition. At the surface of the weld metal bead, where no signs of the former K layer remain, all the increase in hardness imparted by the former K layer is erased. In the hottest portions of the HAZ, where estimated temperatures [10] reached above about 1200 °C the decomposition structure is comprised of the 3–5 μm size cells which are supposedly a mix of coarse M_7C_3 particles and carbon-depleted austenite, the hardness is reduced to 500–800$HV_{0.05}$. In the cooler regions of the HAZ, decomposition of the K layer occurs on a much finer scale and the microstructures consist of a <3 μm thin layer of <1 μm size cells or particles overlaid on a 25–30 μm depth of decorated slip lines and hazy, submicron size particulate structure, presumably largely $M_{23}C_6$. For this fine decomposition structure, the surface hardness can remain unchanged at 1000–1200$HV_{0.05}$, as in traverses A and C, or can be reduced to 700–800$HV_{0.05}$, as in traverse B. Traverse B was in a hotter region and its carbide particles might be a little larger. At 30–70 μm depths, where the decorated austenite grain boundaries reign, the hardness is about 200$HV_{0.05}$, the same as that for the annealed base alloy. It is cautioned that these hardness data are qualitative, and those for the 3–5 μm cell structure, although reproducible, are somewhat less reliable than those for the finer structures and the undecomposed layer. The measured hardness value of a composite of hard carbide particles in a soft austenite matrix will be affected by the number of particles in the small volume probed by the indenter. Because of the need to use small indentations of less than about 15 μm diagonal width to stay within the K layer, relatively few carbide particles are involved in the tests on the 3–5 μm cell structure.

4.2. Irradiated specimens

The above discussion of thermal decomposition and softening of the K layer, particularly the effects of size of the decomposition products, is relevant to the findings for the irradiated specimens where no radiation-induced softening was found. The irradiation temperature of 60–100 °C is quite low in terms of the absolute melting temperature of the steel, and if any irradiation-induced decomposition products were created from the carbon-supersaturated austenite they would be very small, much less than 1 μm. Depending on the degree of decomposition, some carbon might remain in supersaturated solid solution. Such a very fine decomposition microstructure might not show much, or any, change in hardness. Therefore, the fact that no irradiation softening was detected in the hardness tests is ambiguous. It could mean that no significant decomposition of the K layer occurred or decomposition did occur but the products were too small to measurably reduce the hardness value. The results are further confounded by the conflicting involvement of irradiation hardening which is strongly evident in the non-Kolsterised specimens, and which seemingly contributes to the hardness of the K layer, too. Irradiation hardening would tend to camouflage any radiation-induced softening.

This irradiation exposure of 1 dpa is shorter than the lifetime exposure of 5 dpa planned for the SNS target vessel. Nevertheless, a dose of 1 dpa is meaningful in terms of the vessel lifetime because the effects of irradiation on mechanical properties of austenitic stainless steels tend to saturate at doses above about 0.1 dpa [11,12]. The tensile yield strength at 1 dpa is little different from that at 5 dpa. Since hardness scales with yield strength, it is reasonable to suppose that the hardnesses measured in the present work are reasonably close to those for a 5 dpa exposure. Therefore, the absence of radiation softening of the K layer after a 1 dpa exposure will imply little or no softening at 5 dpa. The present irradiation was conducted in a steady mode, not in a pulsed mode that would more closely simulate a SNS exposure, and it does not include the generation of high helium and hydrogen contents expected in the SNS target vessel. However, the irradiated properties data bases do include data for pulsing and high gas contents, gathered for fusion reactor applications. Their effects are small compared to the dose effects. From the bulk radiation effects aspect, irradiation of the vessel to doses of 1 dpa and 5 dpa portends no fatal problems. Unfortunately, what is not covered in the fusion reactor program data base, and is not addressed in the present paper, is the question of liquid cavitational pitting at 5 dpa under high energy pulses. That could be a life-limiting problem. It requires further laboratory experiments or, more desirably, post-irradiation studies of retired target vessels.

4.3. General

These experiments show clearly that when the decomposition products from a carbon-supersaturated austenite layer on stainless steel occur on a

submicron scale the hardness of the aggregate may remain equivalent to that of the undecomposed layer. Whether such a decomposed K layer will retain the same resistance to cavitation pitting as the pristine layer remains to be seen. The answer will require cavitation experiments on K layers that have been decomposed under controlled thermal treatments and are characterized in more detail. For fabrication of the SNS target vessel, most of the welds will be made before the Kolsterising® treatment is applied. In which case, no decomposition products will be involved and the hardness of the K layer on the welds will be the same as on the non-welded parts, as demonstrated in [6]. However, some welding is unavoidable on Kolsterised surfaces in the front end assembly; to reinstate some pitting protection in this region it will be re-Kolsterised after welding.

5. Conclusions

The effects of electron beam welding and neutron irradiation on structural stability and related hardness changes in the surface layer of 316 austenitic stainless steels that was solution hardened by a commercial carburization treatment are described. In welded specimens of 316L steel, the former carburized layer and its high hardness are eliminated in the weld metal. In the weld HAZ, thermal decomposition of the layer occurs. The hardness of the layer in the HAZ depends on the heat distribution and the size of the thermally-formed carbide particles. When the particles are of submicron size the hardness is not reduced. In carburized specimens of annealed and 20% cold-rolled 316LN steel that were neutron irradiated to 1dpa at 60–100 °C, no softening of the K layers was found. Instead, the hardness of the K layers was increased by 2–12%, compared to increases of 81% and 43% for the annealed and 20% cold-rolled substrate materials, respectively. Optical microscopy examinations of the surfaces of the as-Kolsterised-and-irradiated specimens revealed no signs of decomposition attributable to irradiation. The resistances of a decomposed K layer and a re-Kolsterised decomposed K layer to liquid cavitation pitting remain to be demonstrated.

Acknowledgements

This research was sponsored by US Department of Energy, the Office of Basic Energy Science, under Contract DE-AC05-00OR22725 with UT-Battelle, LLC. The authors thank Dr M.L. Santella for providing information on the phase equilibrium during welding process, D. Lousteau and S. Chae for providing the Kolsterised nose pieces, D.A. Frederick for making the welds, and J.R. Mayotte for metallography. The authors also express special thanks to Drs L.K. Mansur, S.J. Pawel, and S.J. Zinkle for their technical reviews and thoughtful comments.

References

[1] T.A. Gabriel, J.R. Haines, T.J. McManamy, J. Nucl. Mater. 318 (2003) 1.
[2] T.E. Mason, D. Abernathy, J. Ankner, A. Ekkebus, G. Granroth, M. Hagen, K. Herwig, C. Hoffmann, C. Horak, F. Klose, S. Miller, J. Neuefeind, C. Tulk, X.-L. Wang, AIP Conf. Proc. 773 (2005) 21.
[3] F.G. Hammitt, Cavitation and liquid impact erosion, in: ASME Wear Control Handbook, American Society of Mechanical Engineers, 1980, p. 161.
[4] C.M. Hansson, I.L.H. Hansson, Cavitation erosion, in: ASM Handbook, Friction, Lubrication, and Wear Technology, vol. 18, ASM International, 1992, p. 214.
[5] Kolsterising®, a hard copy of a CD ROM distributed by Bodycote Metal Technology, August (2001); and some hard-copy fliers; and Bodycote's web page: <http://internet.bodycote.org/kolsterising/>.
[6] K. Farrell, E.D. Specht, J. Pang, L.R. Walker, A. Rar, J.R. Mayotte, in: Proceedings of the 6th International Workshop on Spallation Materials Technology, Kanagawa, Japan, November 30–December 5, 2003, J. Nucl. Mater. 343 (2005) 123–133.
[7] J.R. Holland, L.K. Mansur, D.I. Potter (Eds.), Phase Stability during Irradiation, Proceedings of a Symposium Sponsored by the Nuclear Metallurgy Committee at the Fall Meeting of the Metallurgical Society of AIME, Pittsburgh, Pennsylvania, October 5–9, 1980, The Metallurgical Society of AIME, Warrendale, PA, 1981.
[8] K.C. Russell, J. Nucl. Mater. 206 (1993) 129.
[9] F. Carsughi, H. Derz, P. Ferguson, G. Pott, W. Sommer, H. Ullmaier, J. Nucl. Mater. 264 (1999) 78.
[10] M.L. Santella, K. Farrell, Thermal decomposition of carburized surfaces in 316 stainless steel during welding, report in preparation.
[11] J.E. Pawel, A.F. Rowcliffe, G.E. Lucas, S.J. Zinkle, J. Nucl. Mater. 239 (1996) 126.
[12] K. Farrell, T. S Byun, J. Nucl. Mater. 296 (2001) 129.